



Search for $X \rightarrow ZZ$ with 3 fb^{-1} and Forward Tracking

The CDF Collaboration
URL <http://www-cdf.fnal.gov>
(Dated: January 1, 2009)

We report on an updated search for anomalous production of Z pairs through a new massive resonance X in $2.5\text{--}2.9 \text{ fb}^{-1}$ of $p\bar{p}$ collisions at $\sqrt{s} = 1.96 \text{ TeV}$ using the CDFII detector at the Fermilab Tevatron. To the four-electron channel of the previous search, we have included channels where the Z bosons decay to muons or jets. Muons are not a straightforward extension of the earlier analysis—the quartic dependence on lepton efficiency means the standard tracking and muon reconstruction techniques are very inefficient, and sensitivity optimization for any recorded muon signal required not only judicious choice of kinematic criteria, but development of more efficient tracking algorithms and muon identification. Predicting the dominant backgrounds in each channel using sideband data samples, we observe no excess for $M_X > 300 \text{ GeV}$ consistent with signal and set limits using a Randall-Sundrum graviton acceptance that are 7–20 times stronger than the previous world’s best limit on resonant ZZ production.

Preliminary Results for Winter 2009 Conferences

I. INTRODUCTION

This note describes a search for a new particle X produced in $p\bar{p}$ collisions at $\sqrt{s} = 1.96$ TeV via its decays to two Z bosons. ZZ processes have been well-studied at the LEP experiments[1], which observed no significant deviation from the Standard Model expectation up to an e^+e^- center-of-mass energy of 207 GeV. However, the LEP data can place only indirect constraints on heavier, resonant ZZ production [2], and direct production constraints at high ZZ masses (e.g. above 300 GeV/ c^2 as considered here) must be probed at hadron colliders. This search uses 2.5–2.9 fb $^{-1}$ of collision data from the CDFII detector at the Fermilab Tevatron to improve the previous world’s best limit on massive ZZ production, our published search for $X \rightarrow ZZ \rightarrow eeee$ with 1.1 fb $^{-1}$ [3]. We add the $eejj$ and $\mu\mu jj$ channels, which drive the new limit at very high X masses where their background is negligible, and the $ee\mu\mu$ and $\mu\mu\mu\mu$ channels, which contribute to the limit at intermediate masses where the $Z + \text{jet(s)}$ backgrounds are large. The latter channels motivate our development and use of new general-purpose algorithms to extend the charged particle acceptance of the CDF detector.

The CDFII detector is described in detail in [4]. Section II summarizes our data sample and event selection criteria, Section III describes our estimation of the dominant backgrounds solely from the data, and Section IV reports the results.

II. DATA SAMPLE & EVENT SELECTION

The analysis uses 2.5–2.9 fb $^{-1}$ of data collected between March 2002 and April 2008 via a $E_T > 18$ GeV electron trigger or a $p_T > 18$ GeV muon trigger. From this dataset we select events offline with a reconstructed electron or muon satisfying the corresponding trigger requirements, another lepton of the same type satisfying very relaxed or track-only identification criteria, and then either two additional relaxed leptons or two jets. After identifying the events containing the first dilepton pair using the nominal CDF event reconstruction software, we reprocess these events with a revision of the software which includes more efficient forward tracking algorithms, then select the second pair of final states from the reprocessed data.

The electron criteria listed in Tables I through III are nearly identical to the published $eeee$ analysis. The relaxed criteria require either an isolated calorimeter cluster with energy primarily in the EM compartment or, to recover acceptance from gaps between calorimeter modules, an isolated track. The relaxed muon criteria listed in Table IV require an isolated track satisfying basic track quality criteria and minimal energy in the calorimeter. These tracks may have matching muon chamber stubs, but a stub is required only for the trigger muon. Jets must satisfy the criteria in Table V. Jet energies are corrected for instrumental effects [5].

The relaxed selections increase the single Z yield at the cost of more background than the standard CDF lepton selections, as shown in comparisons of the dilepton mass spectra consisting of a trigger lepton and either a standard or relaxed lepton (Figures 1 and 2.) The larger backgrounds can be easily suppressed with the double Z mass requirement.

The increase in muon acceptance due to the new $|\eta| > 1$ tracking algorithms is demonstrated in Figure 3. Reprocessing all events in an arbitrary 7% subset of the analysis dataset, the Z peak yield from the dedicated forward tracking algorithms increases by more than a factor of two, corresponding to an $\mathcal{O}(10\%)$ increase in the total Z yield. The procedure described earlier in this section, which is fully efficient for signal events, obviates reprocessing of the full dataset.

After selecting four final states, we identify the optimal $llll$ or $lljj$ pairing for each event (if any.) Any two final states must have minimum separation in the $\eta - \phi$ plane of 0.2. For the four-lepton channels, we choose the combination which minimizes a χ^2 variable quantifying consistence between the dilepton masses and the Z pole mass,

$$\chi_{ZZ}^2 = \frac{(M_Z^{(1)} - 91.187 \text{ GeV})^2}{\sigma_{M^{(1)}}^2 + \sigma_\Gamma^2} + \frac{(M_Z^{(2)} - 91.187 \text{ GeV})^2}{\sigma_{M^{(2)}}^2 + \sigma_\Gamma^2}$$

where $\sigma_{M^{(i)}}$ is the detector mass resolution computed from the lepton measurements and σ_Γ accounts for the lineshape of the Z . For the $lljj$ channels, we choose the highest two E_T jets and the dilepton pairing which minimizes the first term of the equation above. We then require $M_Z > 20$ GeV for each pairing and, for the dijet channels, $\chi_Z^2 < 25$. We *a priori* define our signal region to be $M_X > 300$ GeV (so as to avoid most Standard Model backgrounds) and either $\chi_{ZZ}^2 < 50$ (for $llll$ modes) or $65 < M_{jj} < 120$ GeV (for $lljj$ modes).

TABLE I: Central Electron Identification Criteria

Selection Criteria	Trigger (CEM)	Relaxed (CEM)
$E_T(\text{GeV})$	> 20	> 5
$ \text{Track } z_0 \text{ (cm)}$	< 60	< 60
Had/EM	$< 0.055 + (0.00045 \times E)$	$< 0.055 + (0.00045 \times E)$
$\text{Isol}^{\text{cal}}/E^{\text{cal}}$	< 0.2	< 0.2
LshrTrk	< 0.4	
Track p_T (GeV/c)	> 10	

TABLE II: Plug Electron Identification Criteria

Selection Criteria	Relaxed (PEM)
$E_T(\text{GeV})$	> 5
Had/EM	< 0.05
$\text{Isol}^{\text{cal}}/E^{\text{cal}}$	< 0.2
$ \eta_{\text{det}} $	< 2.5

TABLE III: Track Electron Identification Criteria

Selection Criteria	Track Electrons
$p_T(\text{GeV})$	> 10
COT Axial Segments	> 3
COT Stereo Segments	> 2
$ \text{Track } z_0 \text{ (cm)}$	< 60
$p_{\text{trk}} / (\text{Isol}_{\text{trk}} + p_{\text{trk}})$	> 0.9
$ d_0 $	$< \begin{cases} 200 \mu\text{m} & \text{silicon} \\ 2 \text{mm} & \text{no silicon} \end{cases}$
ΔR_{EM}^a	> 0.2

^aSeparation in $\eta - \phi$ plane between track and nearest calorimeter electron cluster.

TABLE IV: Muon Identification Criteria

Selection Criteria	
p_T^{trk}	$> 20 \text{ GeV (Trigger) or } > 2, 10 \text{ GeV}^a \text{ (Relaxed)}$
$ \Delta x_{CMU} $	$< 10 \text{ cm (CMUP Trigger Only)}$
$ \Delta x_{CMP} $	$< 20 \text{ cm (CMUP Trigger Only)}$
$ \Delta x_{CMX} $	$< 10 \text{ cm (CMX Trigger Only)}$
$\text{Isol}^{\text{cal}}/p^{\text{trk}}$	< 0.2
E_{EM}	$< 4 + \max(0, 0.0115 * (\frac{E^{\text{trk}}}{\text{GeV}} - 100)) \text{ GeV}$
E_{HAD}	$< 12 + \max(0, 0.028 * (\frac{E^{\text{trk}}}{\text{GeV}} - 100)) \text{ GeV}$
κ/σ_κ^b	> 2.5
$p(\chi^2, \text{ndof})^c$	$> 10^{-10}$
$ z_0 $	$< 60 \text{ cm}$
$ d_0 $	$< \begin{cases} 200 \mu\text{m} & \text{silicon} \\ 2 \text{mm} & \text{no silicon} \end{cases}$

^aThe lower threshold is used for tracks with muon chamber stubs attached.

^bTrack curvature / resolution.

^cTrack χ^2 fit probability.

TABLE V: Jet Identification Criteria

Selection Criteria	
Algorithm	JETCLU 0.4 Cone
E_T^{raw} (GeV)	> 10
$ \eta_{\text{centroid}} $	< 3.64
E_{EM}/E_{tot}	< 0.95
ΔR_{EM}^a	> 0.4

^aSeparation in the $\eta - \phi$ plane between centroids of the jet cluster and the nearest electron cluster.

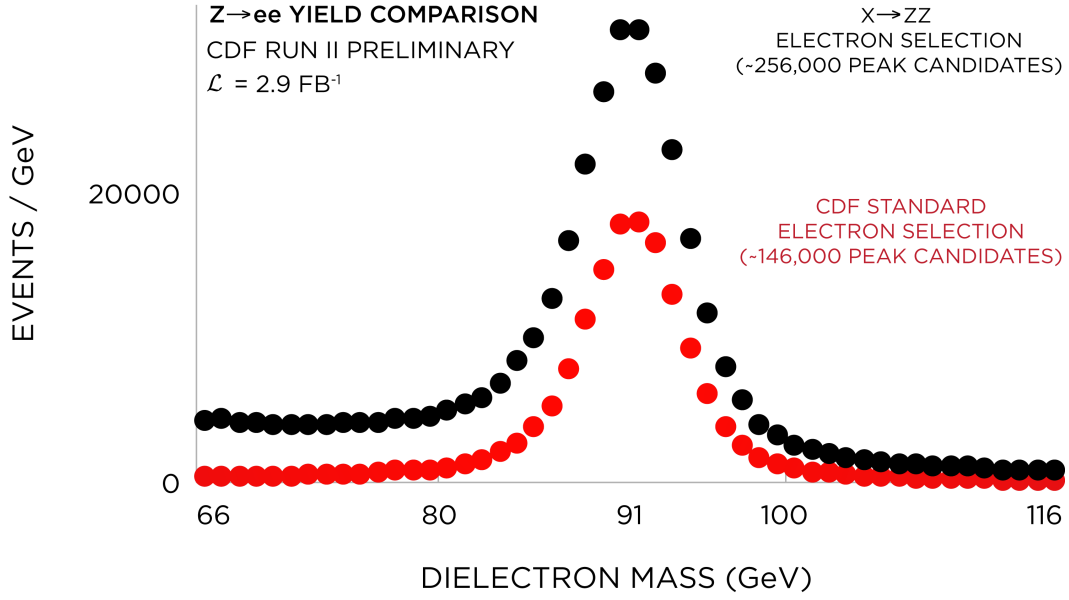


FIG. 1: Dielectron mass distributions for (black) a trigger electron and an electron selected with our selection and (red) a trigger electron and an electron selected with the standard CDF criteria.

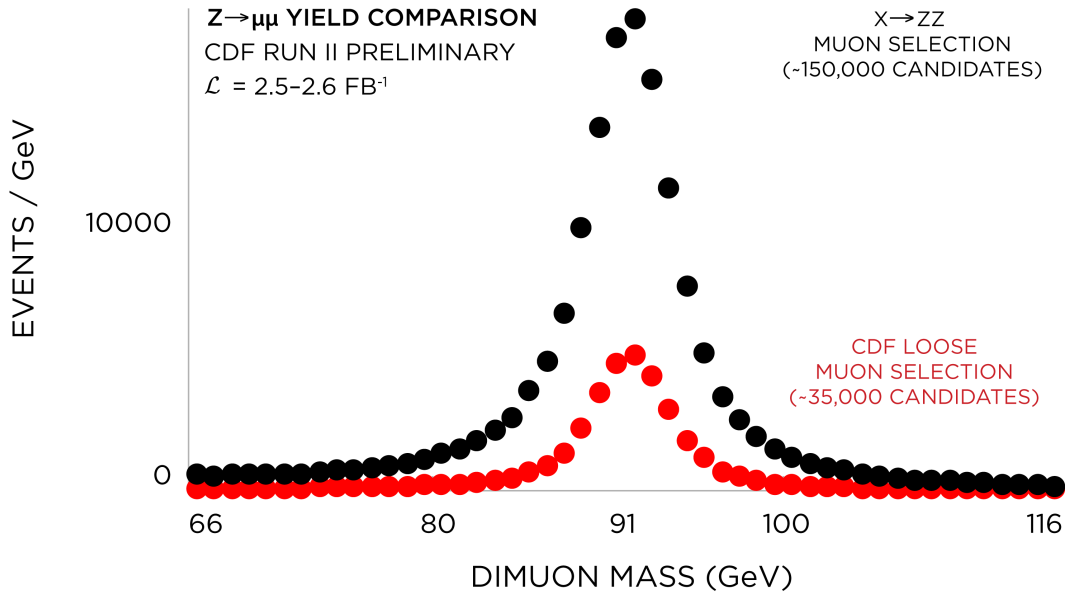


FIG. 2: Dimuon mass distributions for (black) a trigger muon and a relaxed muon and a muon selected with our selection and (red) a trigger muon and a muon with the standard CDF CMUP or CMX criteria.

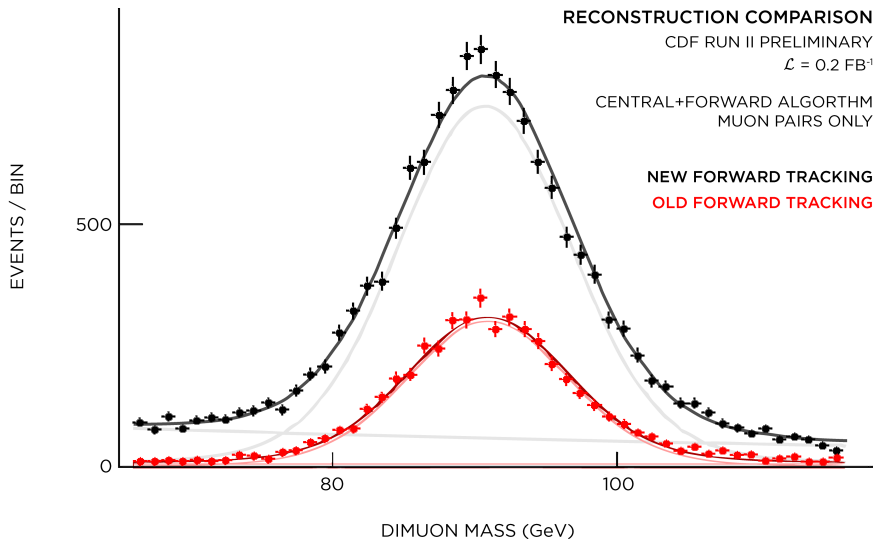


FIG. 3: Mass spectra for the dimuon yield from a 7% subset of the full dataset. Each entry consists of a trigger muon and (red) a muon reconstructed by the dedicated $|\eta| > 1$ tracking algorithms with the standard CDF reconstruction or (black) a muon reconstructed by the new dedicated algorithms.

III. BACKGROUNDS

For both the four-lepton and the dijet channels, the dominant backgrounds at high X mass are a mixture of $Z + \text{jets}$, $W^\pm + \text{jets}$, QCD, and various lower-rate processes resulting in one or more hadrons faking an electron or muon. Only $WZ \rightarrow jjll$, $ZZ \rightarrow llll$, and $ZZ \rightarrow lljj$ processes peak at $\chi_{ZZ}^2 < 50$ or $65 < M_{jj} < 120$ GeV; these are so small that they have only been recently observed at the Tevatron [6, 7]. We use simulation to model these resonant processes and fit sideband data to collectively estimate all non-resonant backgrounds.

The sideband data we fit for the $llll$ backgrounds are the χ_{ZZ}^2 vs. M_X distributions for the four leptons and kinematically similar but orthogonal samples enriched in fakes. We start by constructing the fake samples, replacing either two or three leptons with anti-selected leptons which fail principal ID requirements. Anti-selected electrons must fail the HAD/EM requirement, and anti-selected muons must fail the minimum-ionizing requirements. To further increase statistics, we remove the isolation requirement for anti-selected leptons. We then fit the two- and three-fake $M_X > 185$ GeV, $\chi_{ZZ}^2 < 500$ distributions simultaneously to the empirical form

$$f(\chi_{ZZ}^2, M_X) = M_X^\gamma \cdot e^{\tau \chi_{ZZ}^2}$$

to determine the falling shape of the M_{llll} distribution (the power law parameter γ) and the relationship of the number of events in the $\chi_{ZZ}^2 < 50$ ZZ window to the number in the off-mass sidebands (the exponential decay parameter τ). As background composition and fake rate kinematic dependence varies with trigger dataset and lepton type, we fit these sidebands separately for the $eeee$, $ee\mu\mu$, $\mu\mu ee$ [8], and $\mu\mu\mu\mu$ background shapes. We then normalize this shape to the number of events observed in the $185 < M_X < 300$ GeV four-selected-lepton control region and project it into the blinded signal region.

The sideband data we fit for the $lljj$ backgrounds are events containing a dilepton pair with $\chi_{ZZ}^2 < 25$ and a dijet pair with either $40 < M_{jj} < 65$ GeV or $120 < M_{jj} < 200$ GeV. The M_{jj} spectrum near the Z pole mass is exponentially falling at low M_X but linear for $M_X > 300$ GeV. We simply interpolate the background expectation for $65 < M_{jj} < 120$ GeV from the lower and higher M_{jj} sideband data. To avoid underestimating the background at very high M_X where these sidebands are empty, we make use of the exponential decay of the population of either sideband vs M_X to obtain the numbers used in the interpolation.

IV. RESULTS

Figures 4 and 5 show the combined prediction for all four-lepton channels and for both dijet channels as well as the unblinded data.

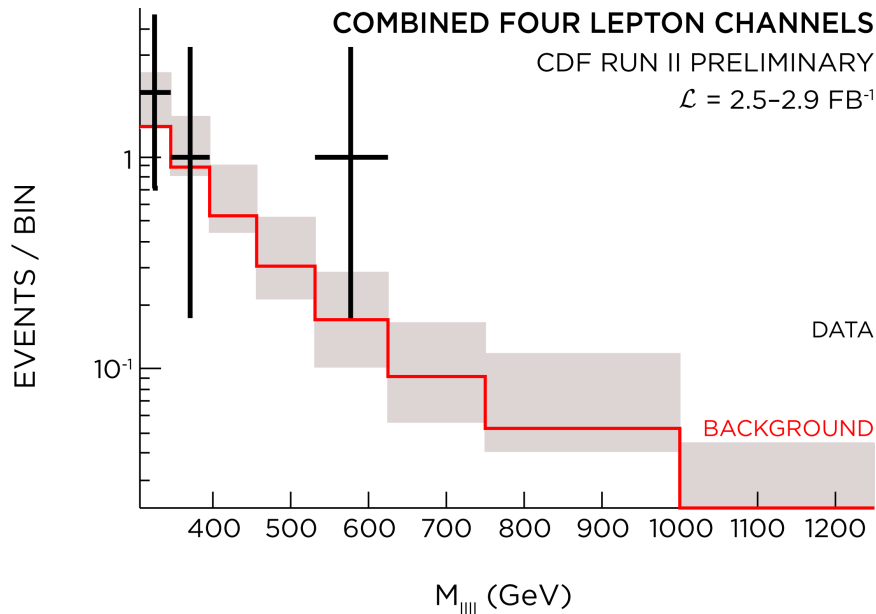


FIG. 4: Prediction and unblinded data for all four-lepton channels combined.

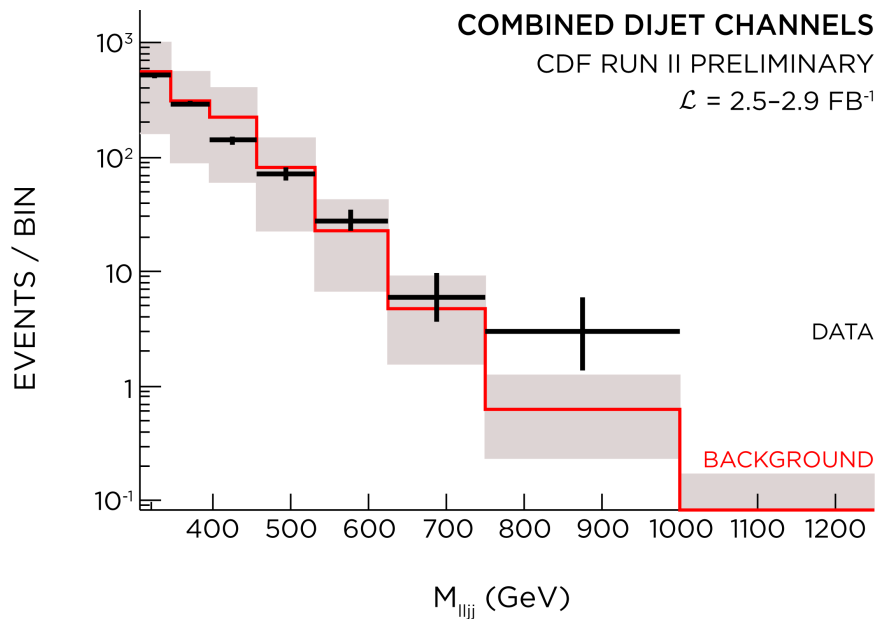


FIG. 5: Prediction and unblinded data for both $lljj$ channels combined.

The spectra provide no compelling evidence for resonant ZZ production. The highest-mass $llll$ event (577 GeV) consists of four muons. The tracking data indicate several of these muons are mismeasured. The highest-mass $lljj$ event (868 GeV) has $M_{ee} = 96.5 \pm 1.3$ GeV and $M_{jj} = 77.8 \pm 6.5$ GeV. Both events are consistent with background expectation.

Absent a signal, we communicate our sensitivity to a ZZ signal process by setting limits with an acceptance from a widely-available HERWIG Monte Carlo process, the spin-2 Kaluza-Klein graviton. The total acceptance times efficiency for this process varies between roughly 40-50% for a given four-lepton channel and between 20-40% for a given dijet channel. We calculate 95% confidence level upper limits as a function of signal mass using Bayesian statistics and a flat prior for the (nonnegative) $X \rightarrow ZZ$ cross section. We assign a 20% uncertainty to the total

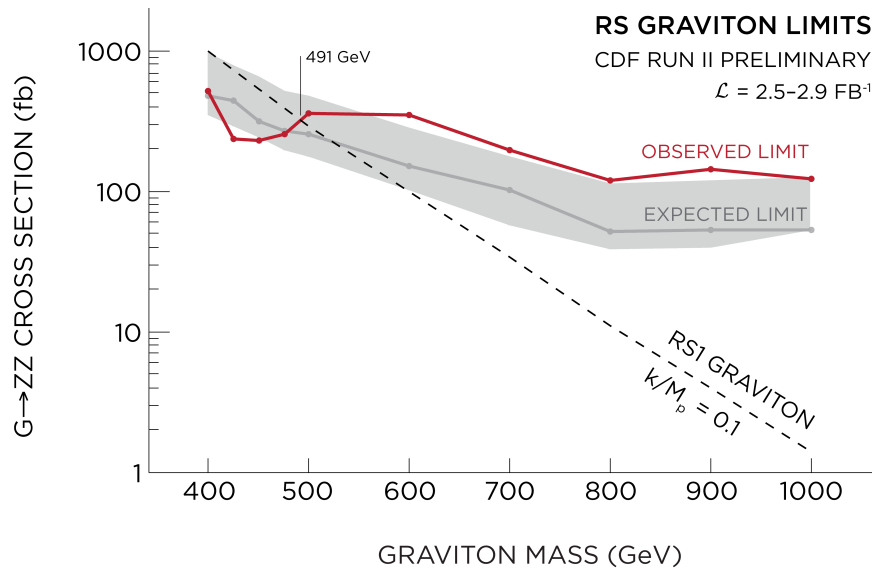


FIG. 6: Cross section limit assuming a spin-2 KK graviton acceptance.

acceptance*efficiency for each channel, over-covering the sum of individual systematic uncertainties in order to simplify the combination. Studies of the individual uncertainties indicate the largest contribution is a 5.9% uncertainty on the luminosity. Figure 6 shows the resultant limit along with the $k/M_p = 0.1$ Randall-Sundrum (RS1) graviton cross section from HERWIG. The present search improves the $\mathcal{O}(4 \text{ pb}^{-1})$ limit of the earlier $eeee$ search by an order of magnitude.

Acknowledgments

We thank the Fermilab staff and the technical staffs of the participating institutions for their vital contributions. This work was supported by the U.S. Department of Energy and National Science Foundation; the Italian Istituto Nazionale di Fisica Nucleare; the Ministry of Education, Culture, Sports, Science and Technology of Japan; the Natural Sciences and Engineering Research Council of Canada; the National Science Council of the Republic of China; the Swiss National Science Foundation; the A.P. Sloan Foundation; the Bundesministerium für Bildung und Forschung, Germany; the Korean Science and Engineering Foundation and the Korean Research Foundation; the Science and Technology Facilities Council and the Royal Society, UK; the Institut National de Physique Nucleaire et Physique des Particules/CNRS; the Russian Foundation for Basic Research; the Ministerio de Ciencia e Innovación, and Programa Consolider-Ingenio 2010, Spain; the Slovak R&D Agency; and the Academy of Finland.

-
- [1] The LEP Collaborations. A combination of preliminary electroweak measurements and constraints on the standard model. *arXiv*, hep-ex, Dec 2006.
 - [2] H Davoudiasl, J L Hewett, and T G Rizzo. Phenomenology of the Randall-Sundrum gauge hierarchy model. *Physical Review Letters*, 84:2080, Mar 2000.
 - [3] CDF Collaboration. Search for new heavy particles decaying to $z_0 z_0 \rightarrow eeee$ in $p\bar{p}$ collisions at $\sqrt{s} = 1.96$ TeV. *Physical Review D*, 78(1), Jul 2008.
 - [4] The CDF II Detector Technical Design Report. *FERMILAB-Pub-96/390-E*, 1996.
 - [5] A Bhatti et al. Determination of the jet energy scale at the Collider Detector at Fermilab. *Nuclear Instruments and Methods in Physics A*, 566:375, Oct 2006.
 - [6] CDF Collaboration. Strong evidence for ZZ production in $p\bar{p}$ collisions at $\sqrt{s} = 1.96$ TeV. *Physical Review Letters*, 100:201801, May 2008.
 - [7] D0 Collaboration. Observation of ZZ production in $p\bar{p}$ collisions at $\sqrt{s} = 1.96$ TeV. *Physical Review Letters*, 101:171803, Oct 2008.
 - [8] The order denotes the trigger required.